Res. Rep. Fac. Eng. Mie Univ., Vol. 11, pp. 95–122 (1986)

Review

Recent Japanese Researches on Reheat Cracking of Steel Welds

Koreaki TAMAKI and Jippei SUZUKI
(Department of Mechanical and Materials Engineering)

(Received September 16, 1986)

Recent studies of the authors and other Japanese researchers on the reheat cracking (the stress relief cracking) in HAZ of Cr-Mo steels including HT80 steels are summarized under the following items. (1)Effect of alloying elements on cracking sensitivity; (a) Combined effect of Cr and Mo was examined and the results were shown in a Cr-Mo contents diagram by contour lines of the critical restraint stress, (b) Effect of V, Ti or Nb on cracking sensitivity from view points of the combined effect with Cr and Mo; The effects of those elements differ largely depending on the basic Cr-Mo contents. The effect of carbide precipitation on cracking sensitivity was discussed. (2) Effect of impurity elements on cracking sensitivity; (a) Magnitude of the effect of several impurity elements were examined. (b) Combined effect of P, Cr and Mo was discussed and the critical P content, below which the steel is prevented from the reheat cracking was proposed. (c) S on cracking sensitivity; The cracking sensitivity of Cr-Mo steel, in which Mn and S contents were varied, was examined and it was found that a small quantity of dissolved sulfur induced harmful effect rather than MnS did. (d) The method of preventing the harmful effect of impurity elements. (4) Effect of other alloying- and impurity elements on cracking sensitivity.

1. Introduction

The reheat cracking or the stress relief cracking occurs occasionally in the heat affected zone of Cr-Mo steels, such as high strength steels and heat resisting steels. This cracking is initiated during the process of stress relief annealing after welding. The crack is initiated mostly in the course of raising the temperature, and propagated along the grain boundary of prior-austenite. Much attention has been paid on the influence of alloying elements on this cracking by the researchers in the world as early in 1960's [1].

As earlier Japanese contributions, Naiki and Okabayashi, and Ito and Nakanishi proposed the cracking sensitivity indexes, ΔG [2] and P_{SR} [3],

respectively for assessing the cracking sensitivity of HT80 high strength steels

$$\Delta G = (\%Cr)+3.3(\%Mo)+8.1(\%V)-2 \quad (1)$$

$$P_{SR}=(\%Cr)+(\%Cu)+2(\%Mo)+10(\%V)+7(\%Nb)+5(\%Ti)-2 \quad (2)$$

Cracking occurs when $G>0$ or $P_{SR}\geqq 0$. Due to their simple expressions, these indexes are conveniently adopted for estimating the cracking sensitivity of HT80 steels.

Another cracking sensitivity index, σrc was proposed [4].

$$\sigma rc=-1.25(Csr-4.7)^{1/2}+20.7 \quad (3)$$

$$Csr=32(\%C)+0.5(\%Cr)+(\%Mo)+11(\%V)$$

$\sigma rc<\sigma w$: cracking occurs. $\sigma rc>\sigma w$: cracking does not occur.

where σrc is the critical stress for producing the reheat cracking, and σw is the stress present in the welded structure. This index differs to above two indexes in including the stress value.

It was pointed out, however, that those indexes could not be applied to the steels of higher Cr and Mo contents, for example, 2 1/4Cr-1Mo and 5Cr-1/2Mo steels [1][3]. And the combined or mutual effect of those elements, which will be naturally expected to exist between two or more elements, is neglected in those simplified equations. Further, the effect of impurity elements is not taken into consideration in those equations.

Recently, several advanced contributions were published in Japan concerning with the influences of alloying and impurity elements on the reheat cracking sensitivity from the view point of the combined action between these elements. In this review, those contributions by the authors and other Japanese researchers were summarized in following sections. (1) Effect of alloying elements, (2) Effect of impurity elements and (3) Effect of other elements.

2. Effect of alloying elements

2.1 Combined effect of Cr and Mo

(1) Cracking test results on 0.02%P steels

Tamaki and Suzuki discussed combined effect of Cr and Mo by a series of experiments [5]-[7]. Steel specimens containing 0 to 5%Cr and 0.25 to 0.5%Mo were prepared as follows. 8 kg ingots were made by melting electrolytic iron, pig iron and ferro-alloys in an induction furnace. Each ingot of 60 mm in diameter was forged into a steel bar of 16 mm in diameter, and the bar was quenched from 950°C and tempered at 700°C. The reheat cracking sensitivity of each steel specimen was evaluated by the magnitude of the critical restraint stress, σAW-crit obtained by a modified implant test [5]. The testing apparatus was composed of an implant test machine, a furnace and a set of measuring devices of stress and temperature. The implant test specimens are shown in Fig.1(a)-(c). The implant and the base metal plate were made of a synthetic steel bar and a commercial HT80 high strength steel, respectively. The implant is inserted in the hole of base metal plate, and a welding bead of 100 mm in length was deposited on the specimen shown in Fig.1(c). A given stress was loaded when the temperature of the heat affected zone fell down to 150°C. Heating began 1 hour after welding finished. The specimen was heated at a rate of 200°C/hr up to 600°C and then held at this temperature for 20 hours. After

this testing, the reheat cracking was inspected at room temperature on the longitudinal cross-section of each implant by a microscope.

The cracking sensitivity was expressed in term of the critical restraint stress, σAW-crit. The amaller σAW-crit is, the more sensitive to cracking the steel is. Four series of Cr-Mo steels of which the P content was kept constant as 0.02% were used. Series A, B, C and D in Table 1 are the specimens of the Mo level of 0.25, 0.5, 1.0 and 1.5%, respectively. The results of cracking test are shown in Fig.2, taking the Cr content as a parameter. The critical restraint stress, σAW-crit is indicated by a curved line which separates the cracking- and no cracking fields. A minimum value of σAW-crit is recognized at about 1.1% Cr for each Mo level.

Table 1 Chemical compositions of Cr-Mo-0.02%P steels [6] (wt%)

No.	C	Si	Mn	P	S	Cr	Mo
A-0	0.20	0.39	1.06	0.02	0.019	0.00	0.27
A-1	0.21	0.37	1.11	0.02	0.019	0.49	0.25
A-2	0.20	0.35	1.15	0.02	0.019	1.03	0.29
A-3	0.19	0.34	1.10	0.02	0.018	1.83	0.27
B-0	0.12	0.42	1.06	0.020	0.020	0.04	0.51
B-1	0.12	0.39	1.06	0.018	0.019	0.58	0.54
B-2	0.11	0.31	0.92	0.020	0.020	0.91	0.52
B-3	0.12	0.34	1.08	0.016	0.019	1.10	0.53
B-4	0.13	0.49	1.22	0.018	0.016	1.83	0.52
B-5	0.14	0.51	1.41	0.017	0.018	2.57	0.53
B-6	0.14	0.41	1.28	0.018	0.018	5.32	0.51
C-0	0.13	0.22	0.91	0.021	0.018	0.01	0.96
C-1	0.14	0.30	1.07	0.018	0.019	0.46	0.92
C-2	0.14	0.27	0.92	0.020	0.018	1.14	0.96
C-3	0.13	0.36	1.19	0.021	0.019	1.44	0.91
C-4	0.13	0.38	1.16	0.019	0.019	2.03	0.93
C-5	0.14	0.45	1.12	0.021	0.019	4.27	0.97
D-0	0.20	0.38	0.99	0.02	0.019	0.01	1.43
D-1	0.18	0.39	0.91	0.02	0.018	0.91	1.51
D-2	0.20	0.38	1.15	0.02	0.019	1.83	1.44
D-3	0.19	0.37	1.07	0.02	0.019	2.73	1.57

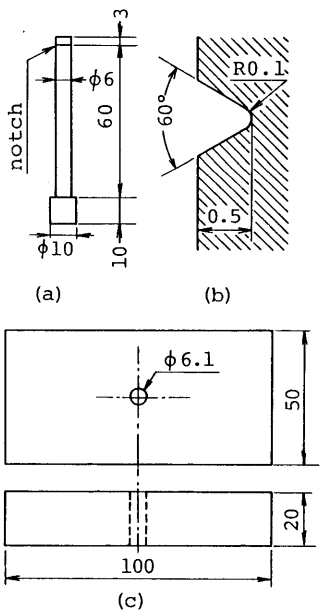

Fig.1 A set of the implant test specimen (a) Implant (b) Details of notched portion (c) Base metal plate [6]

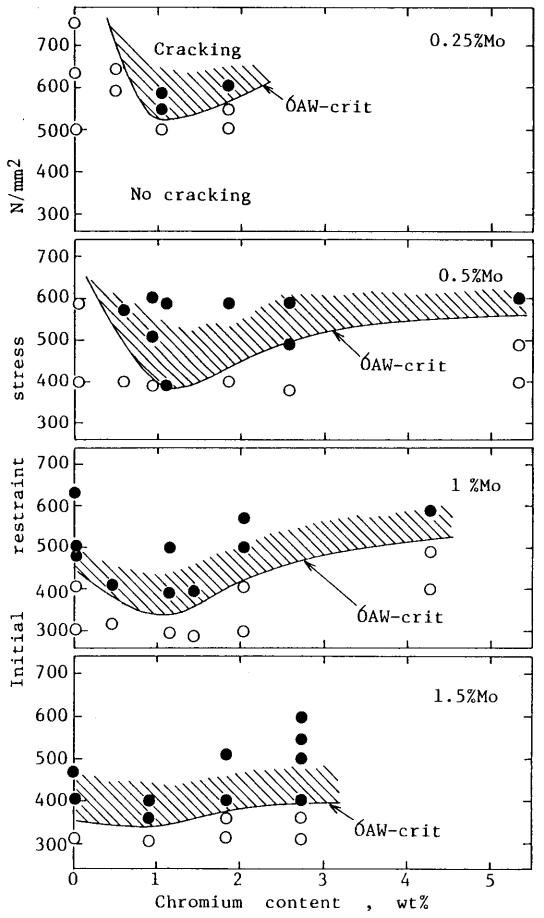

Fig.2 Critical restraint stress, σAW-crit of Cr-Mo-0.02%P steels [6]

On the basis of Fig.2, the contour lines of σAW-crit values are drawn in a Cr-Mo contents diagram as shown in Fig.3(a). This diagram is called hereafter briefly "the σAW-crit contour line diagram". Four Cr-Mo contents fields are recognized in the diagram according to the intensity of cracking sensitivity as Fig.3(b).

Field I; The low Cr and low Mo field, in which the cracking sensitivity is very small. The chemical compositions of 0.5%Mo HT80 steel and 0.5%Mo heat resisting steel correspond to this field.

Field IIa; The low Cr (below about 1%) and medium Mo field, in which the cracking sensitivity increases remarkably with increasing the Cr content. The chemical composition of 3/4Cr-1/2Mo steel belongs to this field.

Field IIb; The high Cr and medium Mo field, in which the cracking sensitivity decreases slightly with increasing the Cr content. The chemical compositions of 2 1/4Cr-1Mo, 2Cr-1Mo, 5Cr-1/2Mo and 9Cr-1Mo steels belong to this field.

Field III; The medium Cr (around 1%) and high Mo (above about 0.5%) field, in which the cracking sensitivity is largest. 1Cr-1/2Mo and 1 1/4Cr-1/2Mo steels have the chemical compositions on the boundary between Field III and IIa.

(2) Cracking test results of 0.01%P steels

The second experiment was made on the specimens containing 0.01%P shown in Table 2. The decrease of the cracking sensitivity brought by reducing the P content was discussed comparing the cracking test result of these steels with that of 0.02%P steels.

The critical restraint stresses, σAW-crit of these steels are shown in Fig.4. σAW-crit values are generally larger for 0.01%P steels than for 0.02%P steels. The difference of σAW-crit for both steels is larger for the chemical compositions around 1%Cr-0.5%Mo, but smaller for other ones.

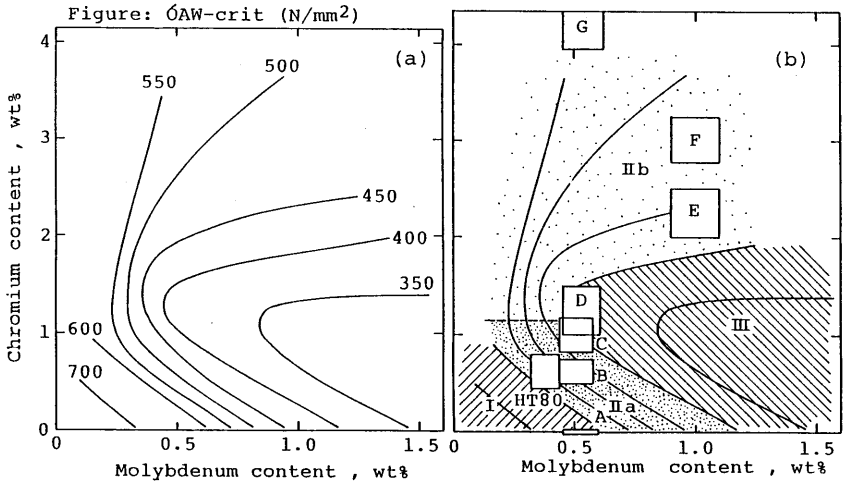

Fig.3 Contour lines of critical restraint stress, σAW-crit of Cr-Mo-0.02%P steels shown in the Cr-Mo contents diagram [6]

Note: A;1/2Mo steel, B;3/4Cr-1/2Mo steel, C;1Cr-1/2Mo steel, D;1 1/4Cr-1/2Mo steel, E;2 1/4Cr-1Mo steel, F;3Cr-1Mo steel, G;5Cr-1/2Mo steel

On the basis of Fig.4, the σAW-crit contour lines diagram of Cr-Mo-0.01%P steels was made as shown in Fig.5(a). The chemical composition fields of I to III are shown in Fig.5(b) as the same way as mentioned in Fig.3(b). Following changes occur by reducing the P content from 0.02 to 0.01%. i) Field I is enlarged covering the higher Cr-Mo contents field. ii) Field IIa moves to the higher Cr-Mo contents side. Therefore, a considerable decrease of cracking sensitivity is expected especially for 3/4Cr-1/2Mo, 1Cr-1/2Mo and 1 1/4Cr-1/2Mo steels when their P contents are decreased from 0.02 to 0.01%.

Table 2 Chemical compositions of Cr-Mo-0.01%P steel [7] (wt%)

No.	C	Si	Mn	P	S	Cr	Mo
LB-0	0.17	0.28	0.53	0.011	0.015	0.02	0.45
LB-1	0.17	0.28	0.57	0.010	0.014	0.46	0.47
LB-2	0.16	0.39	0.75	0.011	0.013	0.99	0.47
LB-3	0.18	0.39	0.84	0.012	0.013	1.98	0.45
LB-4	0.18	0.29	0.80	0.013	0.015	2.63	0.50
LC-0	0.18	0.19	0.56	0.011	0.013	0.01	0.92
LC-1	0.18	0.19	0.89	0.011	0.013	0.48	0.99
LC-2	0.17	0.19	0.91	0.012	0.013	0.96	0.97
LC-3	0.20	0.24	0.87	0.013	0.015	2.03	1.03
LC-4	0.18	0.25	0.84	0.012	0.013	2.19	0.94
LC-5	0.18	0.34	0.64	0.013	0.015	2.89	0.97
LD-0	0.16	0.21	0.55	0.011	0.016	0.00	1.31
LD-1	0.18	0.32	0.82	0.013	0.013	0.97	1.35
LD-2	0.18	0.36	0.62	0.013	0.013	2.01	1.46
LD-3	0.17	0.29	0.28	0.011	0.016	2.65	1.38

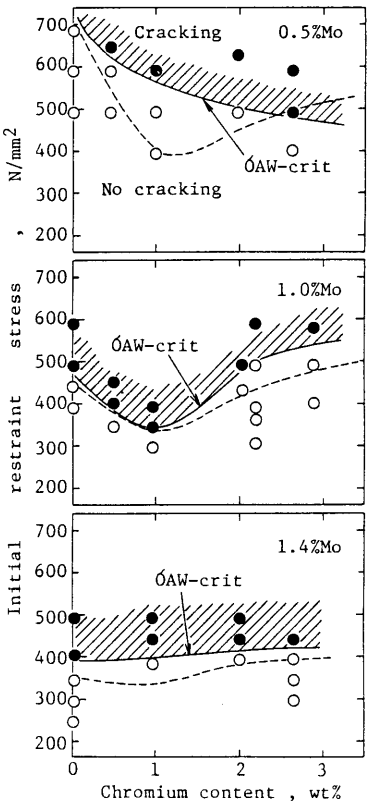

Fig.4 Critical restraint stress, σAW-crit of Cr-Mo-0.01%P steels [7]
Note: Dotted line shows σAW-crit of Cr-Mo-0.02%P steels

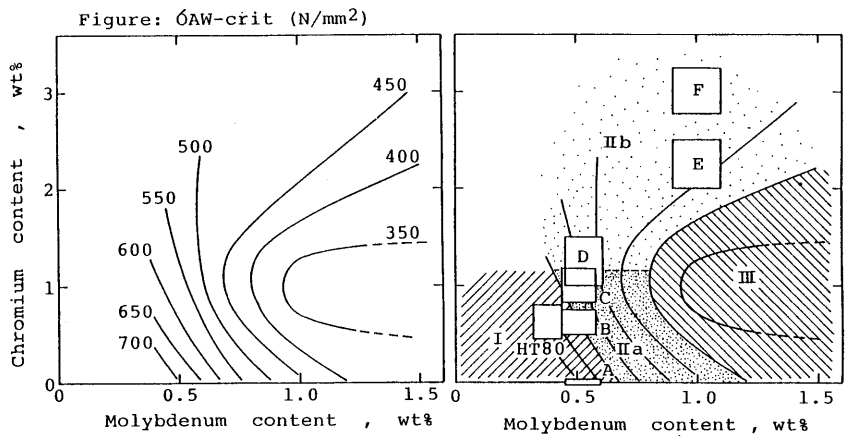

Fig.5 Contour lines of σAW-crit of Cr-Mo-0.01%P steels shown in the Cr-Mo contents diagram [7]
Note: Letters A, B, C,·····; see the note of Fig.3

(3) Relations between Cr-Mo contents-
ΔAW-crit diagram and the cracking indexes

For the steels which contain only two alloying elements, Cr and Mo, the cracking index formulas (1) and (2) become as:

$$\Delta G=(\%Cr)+3.3(\%Mo)-2 \quad (4)$$

$$P_{SR}=(\%Cr)+2(\%Mo)-2 \quad (5)$$

The cracking field was expressed as the field of $\Delta G > 0$ or $P_{SR} \geqq 0$ on the Cr-Mo contents diagram, as shown in Fig.6. The following correspondences can be seen among the four fields of $\Delta G > 0$, $P_{SR} \geqq 0$, Field IIa and III when Cr content is restricted to below about 1%.

i) The field $\Delta G > 0$ corresponds to Field IIa and III ($\Delta AW\text{-crit} < 55 kgf/mm^2$)

ii) The Field $P_{SR} \geqq 0$ corresponds to Field III ($\Delta AW\text{-crit} < 40 kgf/mm^2$)

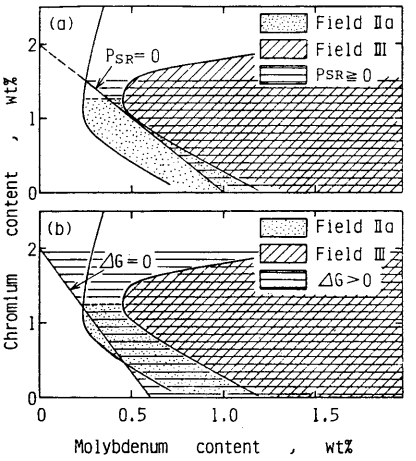

Fig.6 Comparison between the critical restraint stress and the cracking sensitivity indexes, P_{SR} and ΔG [6]

2.2 Combined effect of Cr, Mo and V or Ti

(1) Cracking test results

It is clear that the strong carbide formers, such as V, Ti and Nb affect the cracking sensitivity of steels from the equations of the cracking sensitivity indexes. However, these indexes do not include the combined effect of basic Cr-Mo contents and the third alloying element.

Ito and Nakanishi investigated the effects of V, Ti or Nb on the cracking sensitivity of four typical Cr-Mo steels by using y-groove restraint test specimen [3]. The test results are shown in Fig.7. These elements generally

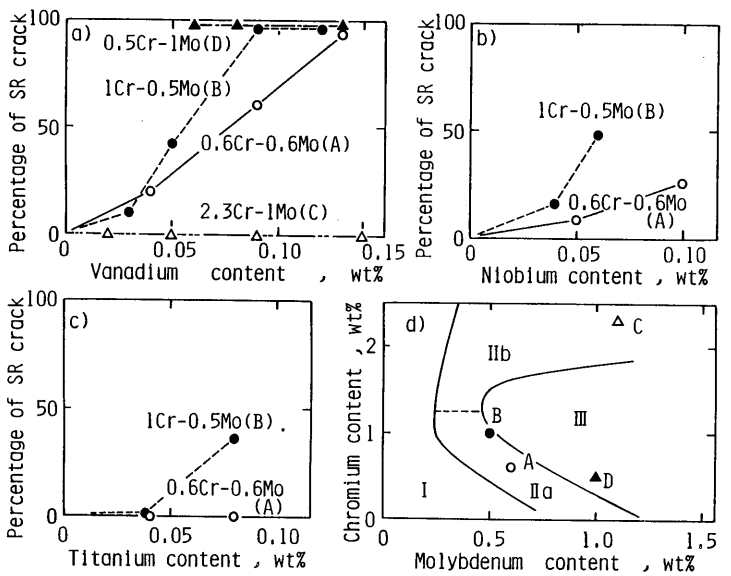

Fig.7 Effects of V, Nb and Ti on the reheat cracking sensitivity [3]

increase the cracking sensitivity, but the magnitudes of their harmful effects depend on the basic Cr-Mo contents. That is, the harmful effect is remarkable in 1Cr-0.5Mo or 0.6Cr-0.6Mo steels and is not recognized in 0.5Cr-1Mo and 2.3Cr-1Mo steels.

Tamaki and Suzuki [8] examined systematically the combined effect of Cr, Mo and V or Ti. The critical restraint stresses were determined for Cr-Mo-0.02%P-0.06%V steels. Chemical compositions of those steel specimens are shown in Table 3. The upper part of Fig.8 shows the cracking test results of the steel groups of 0.25, 0.5 and 0.8%Mo taking the Cr content as a parameter. A solid line and a dotted line denote the critical restraint stresses of Cr-Mo-V and basic Cr-Mo steels (for reference), respectively.

In the case of 0.25%Mo group, the critical restraint stresses of Cr-Mo steels are remarkably decreased by V addition. On the contrary in the case of 0.5 and 0.8%Mo groups, the stress values are decreased only when the Cr content

Table 3 Chemical compositions of Cr-Mo-0.06%V steels [8] (wt%)

No.	C	Si	Mn	P	S	Cr	Mo	V
Va-1	0.20	0.36	1.25	0.02	0.02	0.62	0.27	0.06
Va-2	0.20	0.35	0.97	0.02	0.02	0.86	0.28	0.04
Va-3	0.20	0.34	1.12	0.02	0.02	1.25	0.27	0.06
Va-4	0.18	0.30	1.06	0.02	0.02	1.70	0.25	0.06
Vb-1	0.18	0.34	0.91	0.02	0.02	0.40	0.57	0.05
Vb-2	0.21	0.46	1.04	0.02	0.02	0.67	0.46	0.06
Vb-3	0.21	0.31	0.90	0.02	0.02	0.81	0.51	0.06
Vb-4	0.20	0.36	0.95	0.02	0.02	1.29	0.53	0.06
Vc-1	0.20	0.43	1.01	0.02	0.02	0.01	0.78	0.06
Vc-2	0.20	0.35	1.11	0.02	0.02	0.44	0.79	0.05
Vc-3	0.21	0.42	1.14	0.02	0.02	0.95	0.80	0.06
Vc-4	0.20	0.35	1.19	0.02	0.02	1.33	0.81	0.06
Vc-5	0.18	0.38	1.28	0.02	0.02	2.06	0.75	0.05

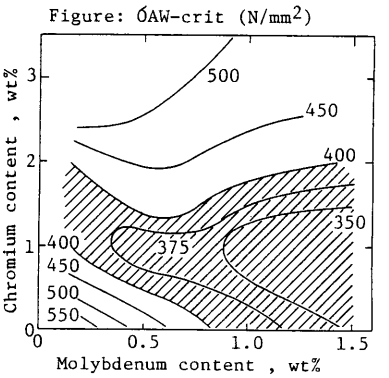

Fig.9 Contour lines of ΔAW-crit of Cr-Mo-0.06%V steels shown in the Cr-Mo contents diagram [8]

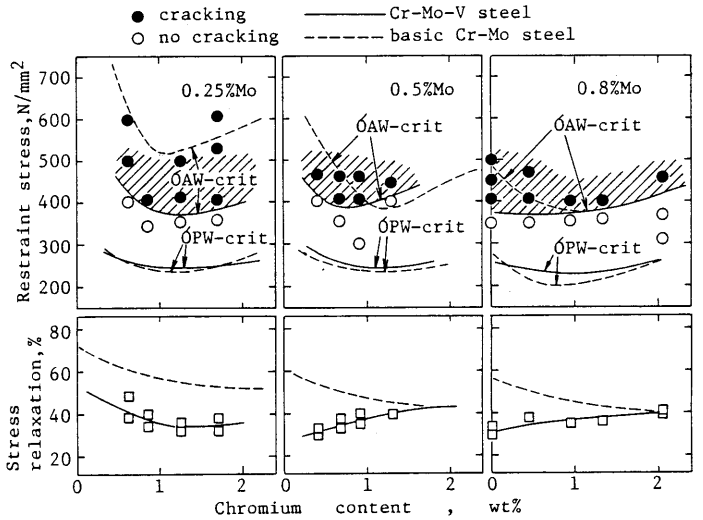

Fig.8 Effect of 0.06% vanadium on ΔAW-crit, stress relaxation and ΔPW-crit of three series of Cr-Mo steels [8]

is smaller than about 1%. Therefore, V increases the cracking sensitivity either when the Mo content is smaller, or when the Mo content is large but the Cr content is small.

Fig.9 is the ÓAW-crit contour lines diagram of Cr-Mo-0.06%V steel. The diagram for basic Cr-Mo steels (Fig.3) changes in appearance with the V addition as follows. i) The Cr-Mo contents field most sensitive to cracking (a shaded field; ÓAW-crit 400N/mm^2) is remarkably expanded to the left hand side (the lower Mo side). ii) Each contour line moves respectively in a parallel direction to the lower Cr side when Cr content is below about 1%.

The critical restraint stresses of Cr-Mo-0.07%Ti steels (Table 4) are shown by solid lines in the upper part of Fig.10. In the case of 0.7%Mo group, Ti decreases clearly the critical restraint stress of the basic Cr-Mo steels for a wide range of the Cr contents. A similar tendency can be seen on the lower Cr side of 0.5%Mo group. But the effect of Ti is little for 0.25%Mo group. As a

Table 4 Chemical compositions of Cr-Mo-0.07%Ti steels [8] (wt%)

No.	C	Si	Mn	P	S	Cr	Mo	Ti
Ta-1	0.17	0.36	0.76	0.02	0.01	0.50	0.25	0.06
Tb-1	0.17	0.24	0.59	0.02	0.01	0.00	0.46	0.06
Tb-2	0.17	0.22	0.71	0.02	0.01	0.46	0.48	0.08
Tb-3	0.18	0.36	0.77	0.02	0.01	0.95	0.49	0.07
Tb-4	0.17	0.19	0.76	0.02	0.01	1.38	0.45	0.08
Tb-5	0.19	0.30	0.79	0.02	0.01	1.64	0.49	0.06
Tc-1	0.17	0.19	0.74	0.02	0.01	0.00	0.71	0.08
Tc-2	0.16	0.25	0.81	0.02	0.01	0.40	0.70	0.07
Tc-3	0.19	0.41	0.69	0.02	0.01	0.98	0.71	0.07

Total N: 0.004-0.006wt%
Soluble N: Ta-1 0.003, others 0.001-0.002wt%

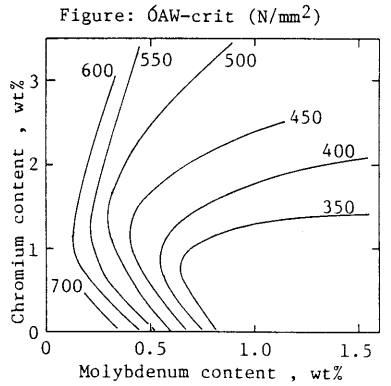

Fig.11 Contour lines of ÓAW-crit of Cr-Mo-0.07%Ti steels shown in the Cr-Mo contents diagram [8]

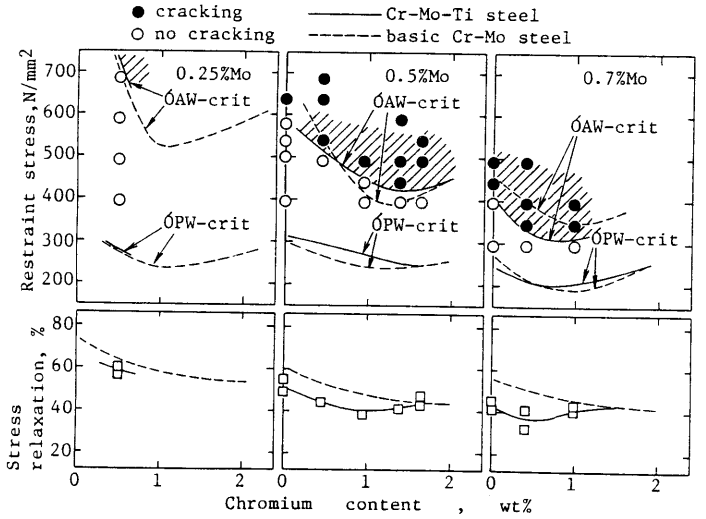

Fig.10 Effect of 0.07% titanium on ÓAW-crit, stress relaxation and ÓPW-crit of three series of Cr-Mo steels [8]

result, Ti exerts a harmful effect only to the steels of larger Mo- and smaller Cr contents.

Fig.11 is the σAW-crit contour lines diagram of Cr-Mo-0.07%Ti steels. This diagram is generally similar in appearance to that of the basic Cr-Mo steels, except for that the taper of each contour line is increased by Ti in the field of larger Mo- and smaller Cr contents.

(2) Effects of V and Ti on stress relaxation

Stress relaxation curves of a V bearing steel (1.7%Cr-0.25%Mo-0.06%V) and the corresponding basic Cr-Mo steel (1.8%Cr-0.27%Mo) are compared in Fig.12. When a stress of 540 N/mm^2 is initially loaded on the basic Cr-Mo steel, a stress relaxation begins to occur by reheating at about 300°C and the stress decreases to as low as 190 N/mm^2 by reheating at 600°C for 1 hour, and reheat cracking dose not occur even after 20 hours at this temperature.

In the case of V bearing steel, a stress relaxation also occurs from about 300°C, but it is much smaller as compared with the basic Cr-Mo steel and therfore, the restraint stress as high as 390 N/mm^2 remains after reheating at 600°C for 1 hour, and the specimen fractures at the marked point in the figure.

From such a comparison, it can be seen that V decreases σAW-crit of the basic Cr-Mo steel mainly by decreasing its stress relaxation.

The values of stress relaxation, R of Cr-Mo-V and Cr-Mo-Ti steels are summarized in the lower parts of Fig.8 and 10 by solid lines, comparing with those of the basic Cr-Mo steels by dotted lines. In this case, the stress relaxation after reheating 600°C for 1 hour was adopted as the stress relaxation value for convenience, it was calculated by the following equation.

$$R600\cdot 1hr = \frac{\sigma AW - \sigma PW600\cdot 1hr}{\sigma AW} \times 100 \quad (\%) \qquad (6)$$

σAW: initial restraint stress, σPW600·1hr: restraint stress after reheating at 600°C for 1 hour.

The stress relaxation of Cr-Mo steel is generally decreased by V and Ti as shown in the figures. And the extent of the decrease of stress relaxation depends largely on the basic Cr-Mo contents. It can be seen that the Cr-Mo

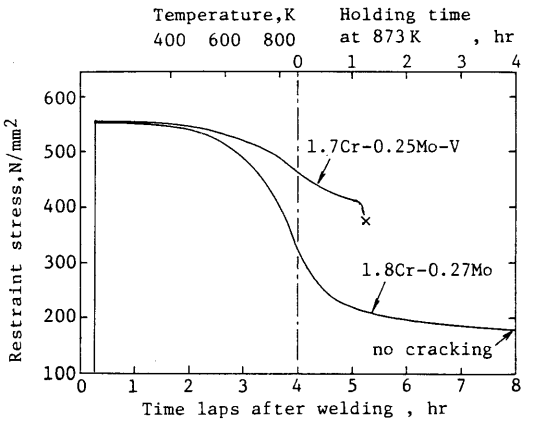

Fig.12 An example of the effect of vanadium on the stress relaxation of a Cr-Mo steel [8]

contents range, in which the stress relaxation is decreased by those elements agrees well with that in which σAW-crit is decreased by them (Fig.8 and 10).

Tamaki and Suzuki [8] pointed out that such decrease of stress relaxation is caused by the precipitation hardening with V_4C_3 or TiC occurring mainly in the heat affected zone.

Another factor which controls σAW-crit is the critical restraint stress at the time when crack initiates, σPW-crit. σPW-crit values were estimated conveniently assuming that the crack would initiate after reheating at 600°C for 1 hour. By changing σAW-crit to σAW in eq.(6) σPW-crit is given as follows:

$$\sigma_{PW\text{-}crit}=\sigma_{AW\text{-}crit}\times\frac{100-R_{600\cdot 1hr}}{100} \qquad (7)$$

σPW-crit values are shown by solid lines in the upper parts of Fig.8 and 10 comparing with those of the basic Cr-Mo steels (dotted lines)[6]. It can be seen that V and Ti hardly vary the σPW-crit values of the basic Cr-Mo steels.

From above considerations, it may be concluded that the increase of cracking sensitivity brought about by V and Ti addition will depend mainly on the decrease of stress relaxation. It should be noted here that such conclusion should be restricted to the effect of small amount of V or Ti. That is, in the case of large amounts (for example above 0.1%) of those elements, their effects of decreasing σPW-crit will not be neglected.

(3) Effects of carbides on stress relaxation

The relation between the decrease in stress relaxation and various precipitates which strengthen the heat affected zone during reheating was examined. The types of carbides and nitrides were identified by an X-ray diffraction on the extracted residues obtained by the electrolytic extraction. Steel specimens used for experiment were oil-quenched from 960°C followed by

Table 5 Carbide types present in tempered Cr-Mo-V steels [8]

steel					A.Q.	tempering temperature and time								decrease of R, ΔR (%)
						500°C		600°C				700°C		
No	Cr %	Mo %	V %	[Cr]+3[Mo]		24 hr	100hr	1 hr	5 hr	24 hr	100hr	24 hr	100hr	
Va-1	0.62	0.27	0.06	1.43	n.p.	M_3C	M_3C	M_3C (V_4C_3)	M_3C (V_4C_3)	M_3C M_7C_3 M_2C V_4C_3	M_3C M_7C_3 V_4C_3 M_2C	M_3C M_7C_3 V_4C_3	M_7C_3 M_3C V_4C_3	20
Va-3	1.25	0.27	0.06	2.06	n.p.	M_3C M_7C_3 V_4C_3	M_3C M_7C_3 V_4C_3	M_3C M_7C_3 (V_4C_3)	M_3C M_7C_3 V_4C_3	M_3C M_7C_3 V_4C_3	M_3C M_7C_3 V_4C_3	M_3C M_7C_3 V_4C_3	M_3C M_7C_3 V_4C_3	20
Vb-1	0.40	0.57	0.05	2.11	n.d.	M_3C V_4C_3	M_3C V_4C_3	M_3C (V_4C_3)	M_3C V_4C_3w	M_3C M_2C V_4C_3	M_3C M_2C V_4C_3	M_3C M_2C V_4C_3	M_3C M_2C V_4C_3	22
Vb-3	0.81	0.51	0.06	2.34	n.d.	M_3C V_4C_3w	M_3C V_4C_3w	M_3C M_7C_3 M_2C V_4C_3	M_3C M_7C_3 M_2C V_4C_3	M_3C M_7C_3 M_2C V_4C_3	M_2C M_3C M_7C_3 V_4C_3	M_3C M_7C_3 M_2C V_4C_3	M_3C M_7C_3 M_2C V_4C_3 $M_{23}C_6$	13
Vb-4	1.29	0.53	0.06	2.88	n.p.	M_3C	M_3C	M_3C M_7C_3 V_4C_3w	M_3C M_7C_3 V_4C_3w	M_7C_3 M_3C	M_7C_3 M_3C	M_7C_3 M_3C	M_7C_3 $M_{23}C_6$	5
Vc-5	2.06	0.75	0.05	4.31	n.p.	M_3C	M_3C	M_3C	M_3C	M_7C_3 M_2C	M_7C_3 M_2C	M_7C_3 $M_{23}C_6$ M_2C	M_7C_3 $M_{23}C_6$	0

Note: ( ); estimated by hardness measurements
n.d.; not determined
n.p.; no diffraction pattern was obtained
w ; a weak diffraction pattern
A.Q.; as-quenched

tempering at 500, 600, and 700°C for 1 to 100 hours.

The results obtained on Cr-Mo-V steels and Cr-Mo-Ti steels are shown in Table 5 and 6, respectively. Carbide types, M_3C, M_2C, M_7C_3 and $M_{23}C_6$ in the tables denote Fe_3C, Mo_2C, Cr_7C_3 and $Cr_{23}C_6$, respectively, in which other metallic elements are dissolved substitutionally. Although V_4C_3, TiC and TiN dissolved also other metallic elements, those original chemical formulas were shown in the tables.

The specimens are arranged in the tables in order of [Cr]+3[Mo] for Cr-Mo-V steels, and in order of [Cr]/[Mo] for Cr-Mo-Ti steels. [Cr] and [Mo] are the contents of those elements (wt%). Carbide types shown in each frame of the tables are arranged in order of the intensity of X-ray diffraction.

(a) Cr-Mo-V steels

V_4C_3, M_3C, M_2C, M_7C_3 and $M_{23}C_6$ precipitate during reheating. Temperature and time at which all the carbides except for V_4C_3 precipitate are quite similar to the results obtained on basic Cr-Mo steels [9]. V_4C_3 precipitates as a stable carbide in wide temperature-time range above 500°C in the steels in which Cr and Mo contents were relatively low. Specimens in which V_4C_3 precipitates agree well with those on which the stress relaxation was considerably decreased.

On the contrary, in the steel of which the stress relaxation is not decreased, a small amount of V_4C_3 precipitates in a very limited temperature-time range. In the steel in which the decrease in stress relaxation is nearly zero, V_4C_3 dose not precipitate throughout the reheating process.

It can be concluded that the decrease of stress relaxation and $\delta_{AW\text{-}crit}$ brought about by V addition are caused by the precipitation hardening with V_4C_3.

(b) Cr-Mo-Ti steel

Ti carbide TiC and nitride TiN are recognized in addition to Cr- and Mo carbides. TiC is present already in the as-quenched specimens of Tc-2, Tb-2 and Tc-3. In these specimens, a clear diffraction pattern of TiC was recognized

Table 6 Carbide types present in tempered Cr-Mo-Ti steels [8]

steel					A.Q.	tempering temperature and time								decrease of R, ΔR (%)
						500°C		600°C				700°C		
No	Cr %	Mo %	Ti %	[Cr]/[Mo]		24 hr	100hr	1 hr	5 hr	24 hr	100hr	24 hr	100hr	
Tc-2	0.40	0.70	0.07	0.57	TiN TiC	M_3C TiC TiN	M_3C TiC TiN	M_3C M_2C TiC TiN	M_3C M_2C TiN TiCw	M_2C M_3C TiN TiC	M_2C M_3C TiN TiC	M_2C M_3C TiC	M_2C M_3C TiC	14
Tb-2	0.46	0.48	0.08	0.96	TiN TiC	M_3C TiC TiN	M_3C TiC TiN	M_3C TiC TiN	M_3C TiC TiN	M_2C M_3C TiC TiN	M_2C M_3C TiC	M_3C TiC	M_3C TiC M_2C	9
Tc-3	0.98	0.71	0.07	1.38	TiN TiC	M_3C TiN TiC	M_3C TiN TiC	M_3C TiN TiC	M_3C TiN TiC	M_2C M_3C TiN TiC	M_2C M_3C TiN TiC	M_2C M_3C TiC	M_2C M_3C TiC	4
Tb-3	0.96	0.49	0.07	1.94	TiN	M_3C TiN	M_3C TiN	M_3C TiN	M_3C TiN	M_2C M_3C TiN	M_2C M_3C TiNw	M_7C_3 M_3C $M_{23}C_6$	$M_{23}C_6$ M_3C M_7C_3	7
Ta-1	0.50	0.25	0.06	2.00	TiN	M_3C TiN	M_3C TiN	M_3C TiN	M_3C TiN	M_3C TiN	M_3C TiNw	M_3C	M_3C	5
Tb-5	1.64	0.49	0.06	3.35	TiN	M_3C TiN	M_3C TiN	M_3C TiN	M_3C TiN	M_3C M_7C_3 TiNw	M_7C_3 M_3C	M_7C_3 $M_{23}C_6$ TiNw	M_7C_3 $M_{23}C_6$	2

Note: see the note of Table 5

even after a large amount of Cr- and Mo carbides precipitate by tempering. The TiC seems to precipitate in tempering stage as well as austenitizing stage. These specimens correspond to those for which the stress relaxation is decreased largely and therfore, $\sigma_{AW\text{-}crit}$ is significantly decreased.

On the contrary, for the specimens Ta-1 and Tb-5 in which TiC does not precipitate, the stress relaxation is hardly decreased.

TiN was observed in all the specimen already in as-quenched state and also in tempered state. But in contrast to TiC, the amount of TiC precipitating during tempering may be very little, because its diffraction pattern was originally weak and disappeared by tempering at higher temperature.

Chemical analyses of steel specimens indicate that the amount of soluble N is very small in Cr-Mo-Ti steel specimens, and therefore, N will be present as nitride in as-quenched condition. This result will support the above conclusion that almost all TiN is produced in austenite state.

From this discussion, it was concluded that the effect of Ti on reheat cracking will be induced mainly by TiC and very little by TiN.

3. Effects of impurity elements

3.1 Comparison of the effects of several impurity elements

Kikuchi and Ohnishi [10]-[13] evaluated the reheat cracking sensitivity of HT80 steels by the amount of plastic deformation at the time of crack initiation, $\Delta lp'$;

$$\Delta lp' = l \cdot (1+\alpha \cdot t) \cdot \frac{\sigma r}{E} - \frac{\sigma tf}{Etf} \qquad (8)$$

where, l is restraint gage length (mm), α is coefficient of liner expansion (10^{-6}/°C), t is temperature at the time of crack initiation (°C), σr is initial stress (Pa), σtf is stress at the time of crack initiation (Pa), E is Young's modulus at room temperature (Pa), and Etf is Young's modulus at crack-initiating temperature (Pa). A synthetic weld thermal cycle was given to the specimen (Fig.13) by using "thermorester" machine, and then the cracking test was performed by the same machine with simulating the stress relaxation

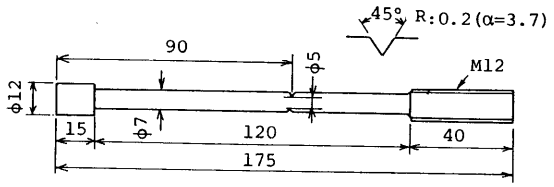

Fig.13 Dimension of reheat cracking test specimen applied with synthetic weld thermal cycle [10]

Table 7 Chemical compositions of steel specimens [14] (%)

Materials	P	S	Sb	As	Sn
HT80	0.020	0.004	0.003	0.003	0.003
P-1	0.044	0.005	0.003	0.002	0.002
P-2	0.096	0.005	0.003	0.003	0.003
S-1	0.024	0.012	0.003	0.002	0.003
S-2	0.023	0.016	0.003	0.002	0.003
S-3	0.023	0.036	0.002	0.002	0.002
Sb-1	0.023	0.004	0.009	0.003	0.003
Sb-2	0.022	0.005	0.038	0.003	0.002
As-1	0.028	0.005	0.003	0.016	0.003
As-2	0.028	0.005	0.002	0.045	0.002
Sn-1	0.021	0.005	0.003	0.003	0.029
Sn-2	0.022	0.004	0.002	0.002	0.055

Other elements (mean values)

0.13C, 0.28Si, 0.93Mn, 0.79Ni, 0.48Cr, 0.44Mo, 0.04V

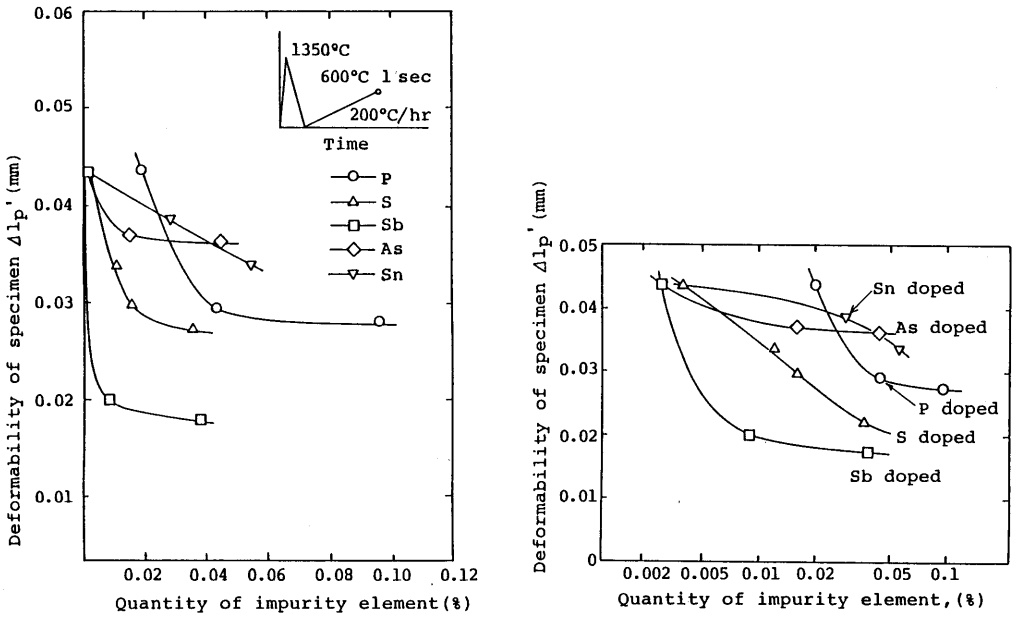

Fig.14 Effects of impurity elements on the deformability of specimen after reheat cracking test [14]

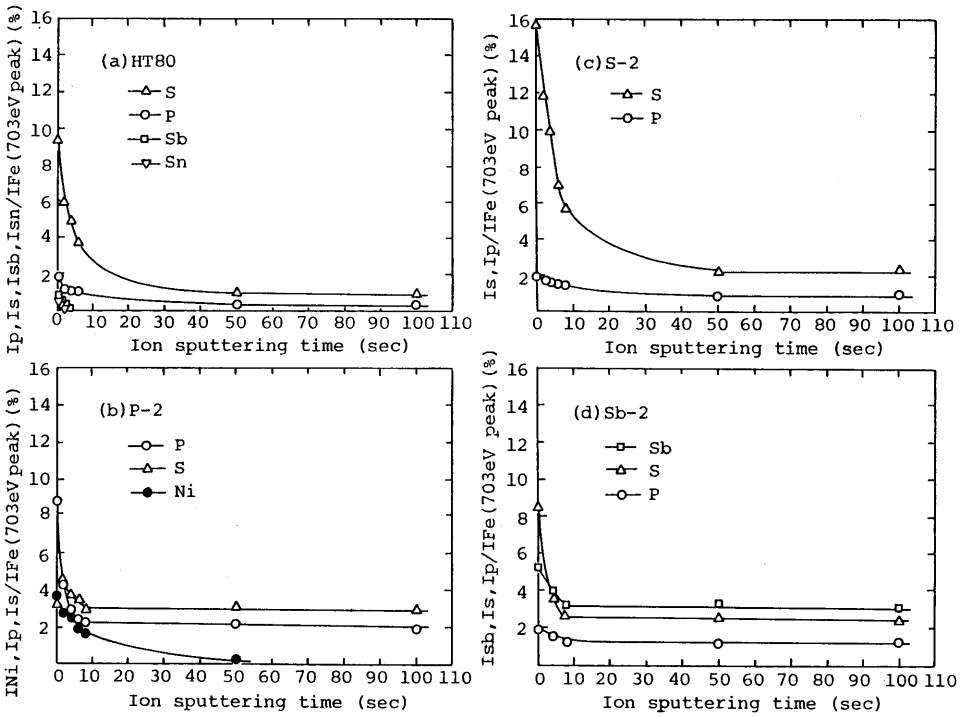

Fig.15 Distribution of impurity elements from grain boundary to grain interior [15]

characteristic of a weldment. Heating rate of 200°C/hr and holding temperature of 600°C were adopted as the standard test condition. They [14][15] compared the magnitude of harmful effects of several impurity elements on reheat cracking sensitivity of a HT80 steel. The chemical compositions of specimens doped with P, S, Sb, As and Sn, repectively, are shown in Table 7. Fig.14 shows the relation between $\Delta lp'$ and the amounts of those elements. Although each of five elements decreases $\Delta lp'$ value, Sb gives most harmful effect; S and P follow it.

Kikuchi and Nakao [15] examined the segregation of impurity elements on the intergranular fracture surface by using the Auger electron spectroscopy. Fig.15 shows the distributions of impurity elements from the grain boundary toward grain interior. This figure indicates that intergranular segregation occurs to a large extent during reheating; the concentrations of impurity elements in the grain boundary is proportional to those in grain interior. The segregation ratio is very large especially for S, P and Sb. It was also clarified that they segregate exclusively within 5 to 10 A from the grain boundaries which consisted of a few atoms layer.

Kikuchi and Nakao explained the mechanism of reheat cracking as follows. Reheating a welded joint having residual stress relieves the stress by converting the elastic strain into a plastic one. If the plastic strain is born by the welded joint as a whole, no reheat cracking may occur because of an extremely small amount of strain, unless the joint material is very brittle. However, when a stress-concentration zone such as a toe of weld exists, plastic deformation may be concentrated locally. The segregation to grain boundary will be accelerated by the concentrated stress, and as a results, the grain boundary will be embrittled. Furthermore, the toe is located in coarse grain zone; the crack-initiating stress of the grain boundary in this zone is smaller than that in fine grain zone. Also, in the coarse grain zone, the flow stress of the grain interior rises on account of hardening by rapid cooling and secondary precipitation hardening, resulting in easy initiation of intergranular cracks without enough plastic deformation.

Matsuzaka and Kirihara [16] also compared the effects of P, Sb, Sn and As in 2 1/4Cr-1Mo steels. The cracking test by constant-loading was carried out on the synthetic HAZ specimens. Their shape and chemical compositions are shown in Fig.16 and Table 8. A special apparatus for measuring the displacement was used (Fig.16). The test results are shown in Fig.17 and 18. They found that the critical displacement and the critical stress to crack initiation could be expressed as a function of the parameter $\bar{X}$, which was formerly proposed by

Table 8 Chemical compositions of materials [16]

Mark of materials	Chemical compositions													
	C	Si	Mn	P	S	Ni	Cr	Mo	V	Sn	Sb	As	C_{eq}*	$\bar{X}$**
A	0.14	0.25	0.57	0.015	0.005	0.05	2.31	0.96	0.03	0.0020	0.0031	0.0050	0.95	17.9
B	0.12	0.31	0.52	0.010	0.009	0.21	2.41	0.97	0.01	0.0080	0.0056	0.0090	0.95	16.9
C	0.13	0.20	0.54	0.013	0.008	0.21	2.18	0.98	0.01	0.0030	0.0007	0.0080	0.91	15.4
D	0.14	0.39	0.50	0.010	0.013	0.05	2.22	0.95	tr.	0.0020	0.0006	0.0010	0.96	11.2
E	0.06	0.26	0.40	0.015	0.015	0.13	2.28	0.94	0.01	0.0140	0.0023	0.0180	0.83	23.6

* $C_{eq}=C+1/6Mn+1/24Si+1/40Ni+1/5Cr+1/4Mo=1/14V(\%)$

** $\bar{X}=(10P+5Sb+4Sn+As)/100$ (ppm)

Bruscato [17] for assessing the sensitivity of temper embrittlement of weld metal.

$$\bar{X}=(10P+5Sb+4Sn+As)/100 \quad \text{(ppm unit)} \qquad (9)$$

3.2 Effect of P

Ikawa and Nakao [18] expressed the reheat cracking sensitivity of steels by the term of deformability. The critical crack opening displacement at the tip of notch, Φc, obtained by tensile test at elevated temperature was used as the parameter to evaluate the deformability. A synthetic HAZ specimen shown in Fig.19(a) was heated up to a test temperature and then fractured by tensile loading. Φc value was determined on one of the notches, at which fracture did not occur, as illustrated in Fig.19(b).

They examined the effect of P on Φc and also intergranular fracture ratio (IGFR) at 600°C in T-1 type HT80 steels shown in Table 9 [19][20]. Synthetic HAZ specimen was pre-heated at 500 and 550°C for 1 to 64 min in order to induce P segregation, and then quenched. It was reheated rapidly up to 600°C and fractured. As the results, Φc values and IGFR are shown in Fig.20(a) and (b). Φc value decreases with increasing the bulk P content; it decreases with

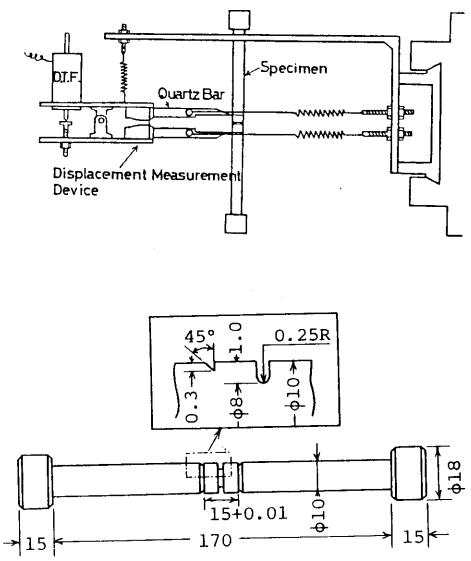

Fig.16 Details of specimen [16]

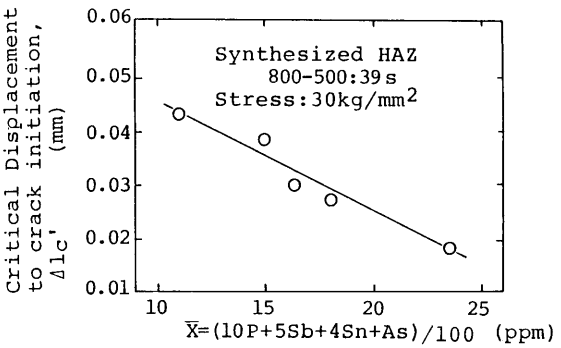

Fig.17 Relation between $\bar{X}$ and critical displacement to crack initiation [16]

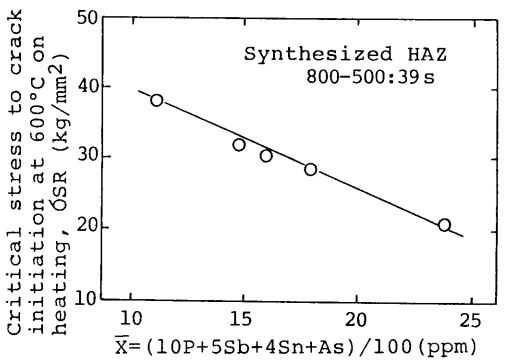

Fig.18 Relation between $\bar{X}$ and critical stress to crack initiation to 600°C on heating [16]

extending the pre-heating time up to 64 min. IGFR increases with increasing the bulk P content and reaches the values of 85 to 100% in 0.094%P steel. Prolonged pre-heating also decreases the IGFR. As another examination, the synthetic HAZ specimen was heated rapidly up to 450°C and then heated with several heating rate up to 600°C, followed by quenching. It was reheated up to 600°C and fractured. The results are shown in Fig.21 [20]. Φc value decreases and IGFR increases with increasing the heating time from 450 to 600°C.

The analyses by Auger electron spectroscopy were carried out on the fracture surface of A80 steel heated at 550°C for 64 min. Phosphorus segregation could be observed on the intergranular fracture surface. Ikawa and Nakao calculated the P concentration at the grain boundary on the basis of the equilibrium segregation theory. McLean [21] has proposed the following equations from that theory.

$$Cgb_{\infty}=Cm\cdot\frac{\exp(\frac{E}{RT})}{1+Cm\cdot\exp(\frac{E}{RT})} \tag{10}$$

$$\frac{Cgbt-Cgbo}{Cgb_{\infty}-Cgbo}=1-\exp(\frac{4D\cdot t}{\alpha^2\cdot d^2})\cdot erfc(\frac{2\sqrt{D\cdot t}}{\alpha\cdot d}) \tag{11}$$

where, Cgb_{∞} is the equilibrium grain boundary concentration of an impurity element attained after

Table 9 Chemical compositions of materials used (%) [20]

Mark	C	Si	Mn	P	S	Ni	Cr	Mo	V	Cu
A80	0.11	0.32	0.78	0.008	0.006	0.97	0.39	0.36	0.033	0.23
L80	0.11	0.32	0.78	0.047	0.008	0.98	0.40	0.37	0.035	0.24
N80	0.11	0.31	0.79	0.094	0.009	0.98	0.39	0.38	0.040	0.23
F80	0.09	0.33	0.84	0.003	0.005	0.93	0.42	0.48	0.035	0.25

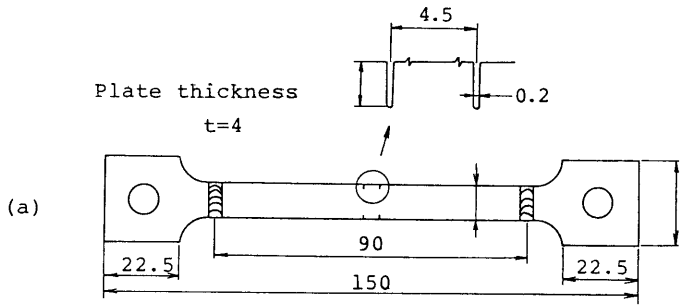

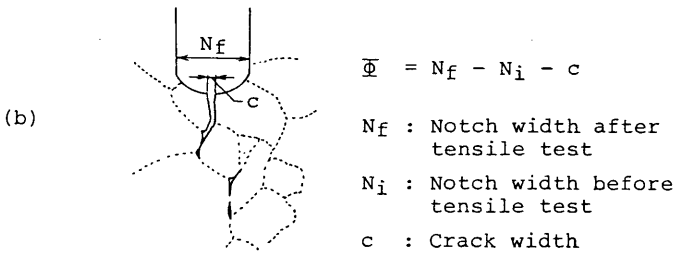

Fig.19 Specimen for measuring Φc and definition of Φc

infinite time, Cm is the grain interior concentration, assumed constant, E is the activation energy for the equilibrium segregation, R is the gas constant, T is the temperature, Cgbt is the grain boundary concentration after time t, Cgbo is the initial grain boundary concentration, α is the ratio Cgb_{∞}/Cm, D is the diffusion coefficient, d is the thickness of the grain boundary and t is the time.

As the result of calculation, in which E=9500 cal/mol was used [20], the relation between IGFR values of all specimens and the P concentration at grain boundary is shown in Fig.22.

Nakao and Nishiyama [22] measured the crack-initiating stress at grain boundary under constant-load. Synthetic HAZ specimen (Fig.23) was heated rapidly up to 400°C and then heated up to 600°C with various heating time. Fig.24 shows the effect of the heating time between 400 to 600°C on the crack-initiating stress at grain boundary (CSGB) of the steel specimens shown in Table 9. CSGB decreases with increasing the heating time and with increasing the bulk P concentration. This result suggests that the P segregation reduces CSGB. Fig.25 shows the relation between CSGB and P concentration at grain boundary which was calculated by using the equations (10) and (11). A clear

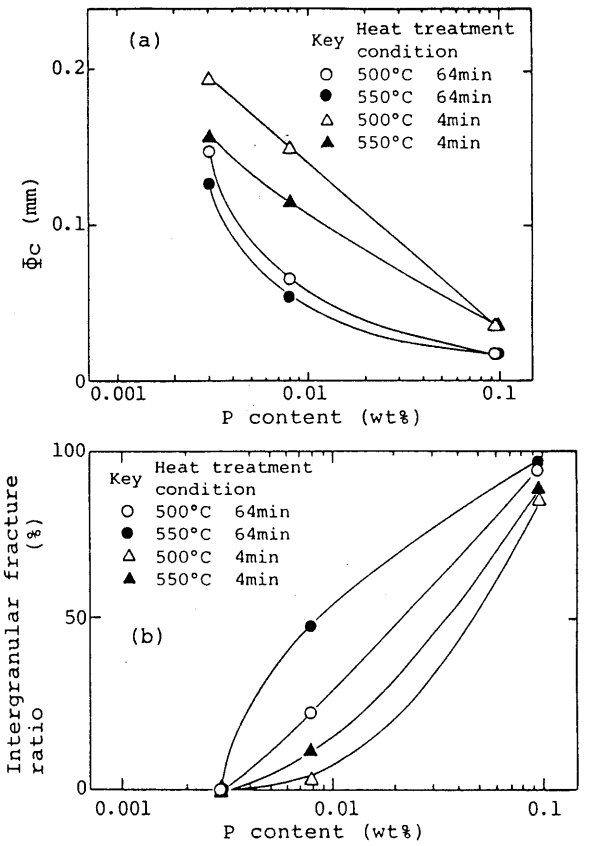

Fig.20 Effect of P concentration and heat treatment consitions on $\bar{\Phi}c$ and intergranular fracture ratio at 600°C in HT80 steels [20]

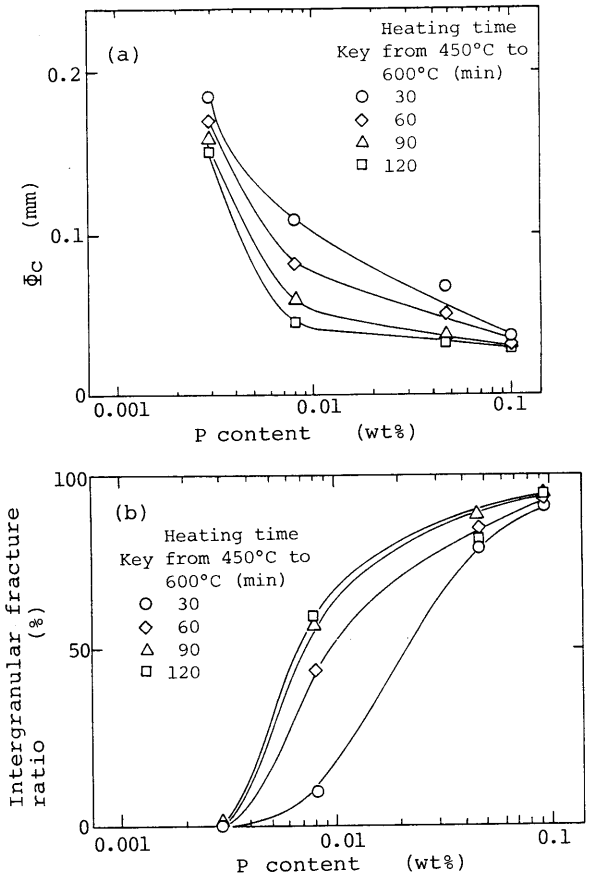

Fig.21 Effects of P concentration and heat treatment conditions on Φ_c and intergranular fracture ratio at 600°C in HT80 steels [20]

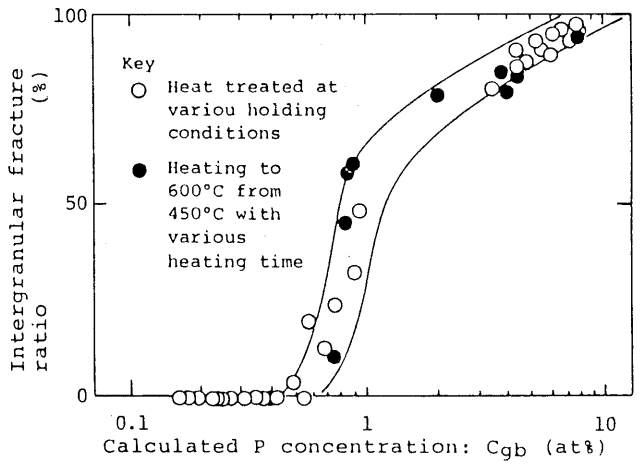

Fig.22 Correlation between intergranular fracture ratio and calculated P concentration at grain boundary (HT80 steel, 600°C) [20]

correlation can be seen between stress and the P concentration at grain boundary.

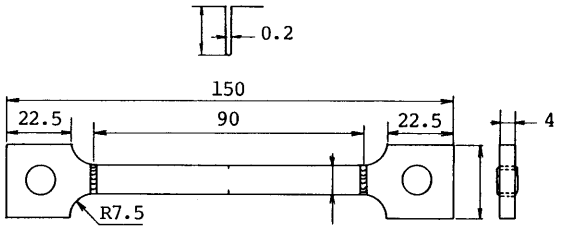

Fig.23 Schematic views of the test specimen [22]

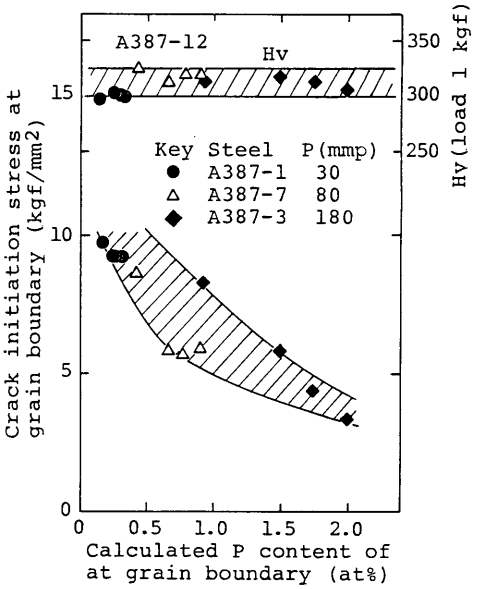

Fig.25 Relations between crack initiation stress at grain boundary and calculated P content at grain boundary [22]

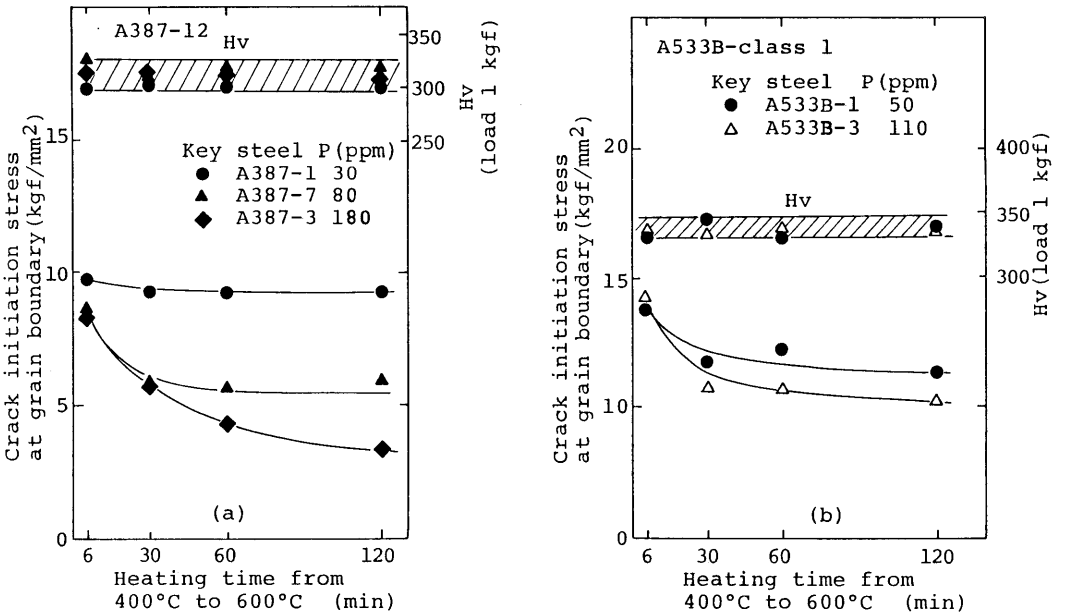

Fig.24 Effect of heating condition on the crack initiation stress at grain boundary in (a)A387-12 and (b)A533B-Cl.1 steel [22]

3.3 Effect of Sb

Nakao and Nishiyama [23] examined the effect of Sb on cracking sensitivity of A387 and A533B steels (Table 10). These steels were normalized and tempered at 650°C for 50 min (A387 steel)or at 670°C for 35 min (A533B steel). Synthetic HAZ specimen shown in Fig.23 [22] was heated rapidly up to 400°C and then heated up to 600°C with various heating rates. The specimen was fractured at -100°C by a Charpy impact test machine. Fig.26 shows the effect of the bulk Sb concentration on the crack initiation stress at grain boundary (CSGB) of A387 steel. CSGB decreases with increasing the heating time and the bulk Sb content.

The effects of the calculated Sb concentration at grain boundary [22] on the crack initiation stress at grain boundary for A387 and A533B steels are shown in Fig.26 and Fig.27, respectively. CSGB decreases with increasing the Sb concentration at grain boundary.

Table 10 Chemical compositions of materials [23] (%)

Mark	C	Si	Mn	P	S	Cu	Cr	Ni	Mo	Sb	Sn	As
A387-1	0.165	0.24	0.63	0.003	0.006	0.11	0.99	0.16	0.50	0.0004	0.0005	0.001
A387-2	0.160	0.25	0.61	0.010	0.007	0.14	1.03	0.15	0.51	0.0050	0.0007	0.003
A387-3	0.162	0.27	0.63	0.018	0.004	0.10	0.97	0.15	0.50	0.0004	0.0005	0.001
A387-7	0.167	0.27	0.62	0.008	0.007	0.16	0.99	0.16	0.49	0.0004	0.0012	0.001
A533B-1	0.183	0.185	1.40	0.005	0.008	-	0.19	0.63	0.557	0.0004	0.0005	0.001
A533B-3	0.19	0.20	1.44	0.011	0.005	-	0.18	0.66	0.543	0.0005	0.0004	0.001

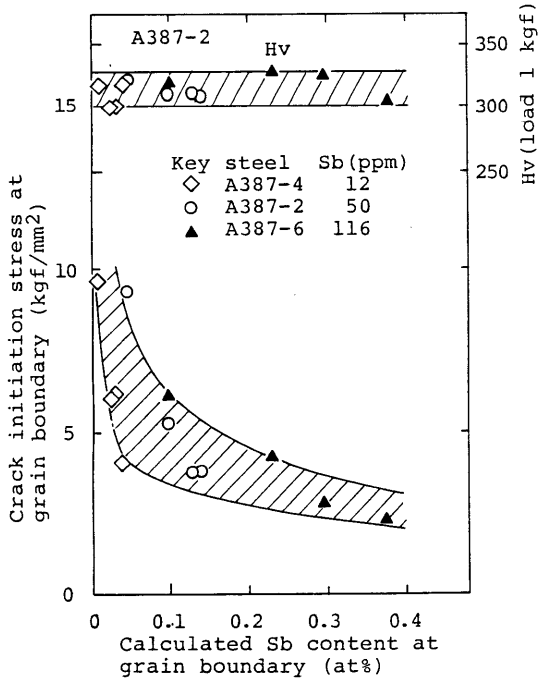

Fig.26 Relation between intergranular crack initiation stress at 600°C and calculated Sb content at grain boundary in A387-12 [23]

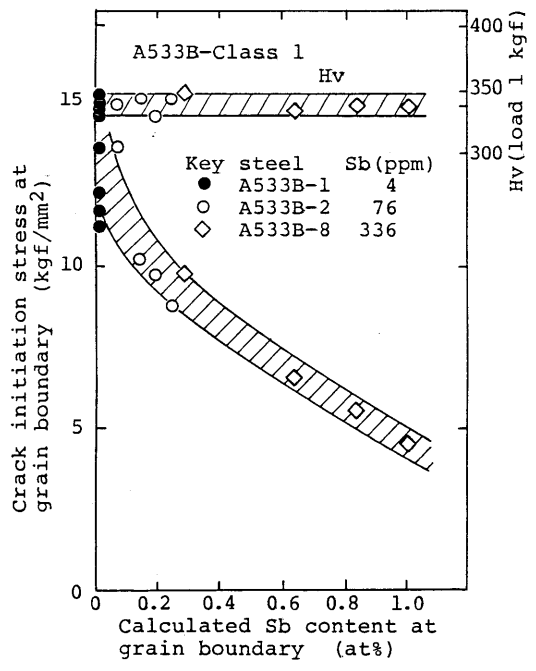

Fig.27 Relation between intergranular crack initiation stress at 600°C and calculated Sb content at grain boundary in A533B steel [23]

3.4 Combined effects of Cr, Mo and P

As previously mentioned in section 2.1, the effect of reducing the P content largely differs depending on the combinations of Cr-Mo contents. From this point of view, Tamaki and Suzuki [7] investigated the effect of P in detail on five Cr-Mo steels; 0Cr-1/2Mo, 1/2Cr-1/2Mo, 1Cr-1/2Mo, 1 1/4Cr-1/2Mo and 2Cr-1Mo steels. Chemical compositions of those steel specimens are shown in Table 11. Their P content were varied from 0.004 to 0.1%. The results of cracking test are shown in Fig.28. A logarithmic scale is used for the abscissa of P content.

In the case of 0Cr-1/2Mo steel (Fig.28(a)), the critical restraint stress is little decreased by increasing the P content from 0.01 to as high as 0.1%,

Table 11 Chemical compositions of five types of Cr-Mo steels containing 0.004 to 0.107%P [7] (wt%)

No.	C	Si	Mn	P	S	Cr	Mo
PA-1	0.17	0.28	0.53	0.011	0.018	0.00	0.45
PA-2	0.16	0.36	0.97	0.013	0.019	0.11	0.48
PA-3	0.12	0.42	1.06	0.020	0.018	0.04	0.51
PA-4	0.17	0.29	0.82	0.031	0.019	0.04	0.49
PA-5	0.18	0.25	0.78	0.085	0.020	0.01	0.48
PB-1	0.16	0.25	0.65	0.006	0.019	0.50	0.48
PB-2	0.17	0.28	0.57	0.010	0.014	0.46	0.47
PB-3	0.12	0.39	1.06	0.018	0.019	0.58	0.54
PB-4	0.17	0.28	0.84	0.060	0.020	0.49	0.50
PB-5	0.17	0.40	0.76	0.094	0.017	0.45	0.51
PC-1	0.17	0.36	1.12	0.006	0.020	1.13	0.47
PC-2	0.19	0.28	0.83	0.008	0.018	1.05	0.46
PC-3	0.16	0.39	0.75	0.011	0.014	0.99	0.47
PC-4	0.12	0.34	1.08	0.016	0.016	1.10	0.53
PC-5	0.19	0.29	0.84	0.021	0.019	1.05	0.45
PC-6	0.18	0.26	0.81	0.096	0.014	0.97	0.43
PD-1	0.18	0.37	1.11	0.014	0.020	1.25	0.49
PD-2	0.16	0.44	1.27	0.023	0.014	1.28	0.47
PD-3	0.17	0.30	0.97	0.063	0.018	1.42	0.49
PD-4	0.16	0.45	1.19	0.098	0.019	1.39	0.50
PD-5	0.17	0.31	0.97	0.107	0.020	1.30	0.42
PE-1	0.20	0.26	0.93	0.004	0.019	2.21	0.84
PE-2	0.18	0.25	0.84	0.012	0.015	2.19	0.94
PE-3	0.20	0.24	0.87	0.013	0.017	2.03	1.03
PE-4	0.13	0.38	1.16	0.019	0.020	1.03	0.93
PE-5	0.18	0.26	0.86	0.102	0.019	1.89	0.85

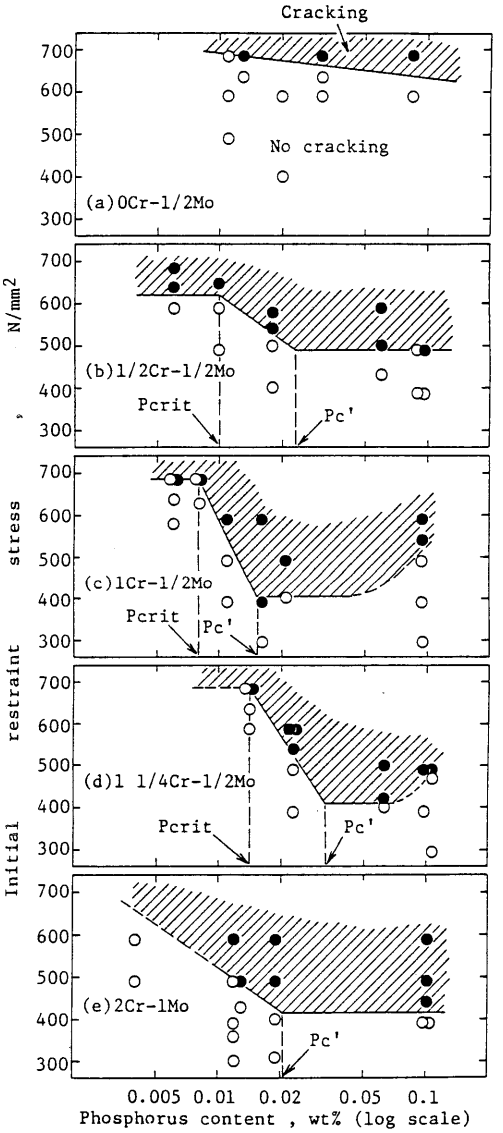

Fig.28 Influence of P on σAW-crit of five types of Cr-Mo steels [7]

that is, the harmful effect of P is hardly recognized for this steel.

In the case of 1/2Cr-1/2Mo steel (Fig.28(b)), the critical restraint stress is large enough in the P content range below 0.01%; it decreases steeply as the P content increases from 0.01 to 0.02%; and dose not decrease any further in the range above 0.02%P. Therefore, there are two critical values of P content, Pcrit and Pc' as shown in Fig.28(b). The lower critical value, Pcrit is regarded as the threshold value or the target value for preventing the reheat cracking by mean of decreasing the P content, and named here "the critical P content". The critical P content of 1/2Cr-1/2Mo steel is 0.01%.

Another critical value, Pc' will be less important from the view point of preventing the reheat cracking, and therefore, the following discussion in this paper is restricted only to Pcrit value.

In the case of 1Cr-1/2Mo and 1 1/4Cr-1/2Mo steels (Fig.28(c) and (d), respectively), the critical restraint stress is varied also in stepwise with the increase of P content. Their Pcrit values are 0.008 and 0.014%, respectively.

Pcrit value of 2Cr-1Mo steel (Fig.28(e)) could not be determined exactly; it will be a value between 0.004 and 0.01%.

In recent investigation, Tamaki and Suzuki [7] revealed that Pcrit value of each steel corresponded closely to a specific P content above which P segregates in a considerable concentration at the austenite grain boundary in the welding stage. P segregation in this stage is further intensified by reheating up to 500°C. Those investigations on the P segregation suggest that Pcrit values of 1/2Mo and 2Cr-1Mo steels, which could not be determined by the cracking test, will be 0.05 and 0.005%, respectively.

4. Effects of sulfide forming elements

4.1 Combined effect of Mn and S

Tamaki, Suzuki et al. [24] examined the combined effect of Mn and S from the following view points; i) the effect of manganese sulfide which prepares the place of crack-initiation, ii) the effect of dissolved S which segregates at the grain boundary and embrittles it. Table 12 shows the chemical compositions of 1Cr-1/2Mo steels, in which S content was varied from 0.02 to 0.1%, whereas Mn content was kept as 0.5 or 1.0%. The reheat cracking test was made at 600, 650 and 675°C by using the implant type testing machine. The test results are shown in Fig.29(a)-(c). Those figures show that; i)The effect of S varies largely depending on Mn level. In the case of 0.5%Mn, the critical restraint stress decreases with increasing S content up to 0.03% and then reaches a constant value for each testing temperature. In the case of 1%Mn, the critical restraint stress decreases a little with increasing S content. ii) The critical restraint stresses of 1%Mn steels are generally much larger than those of 0.5%Mn steels. iii) The testing temperature affects a little on the test results.

Types of sulfide in the as-welded HAZ were determined by X-ray analysis on electrolytically extracted residues. The results are shown in Table 13. Only MnS type sulfide is present in all 8 specimens. The amount of sulfide

(extracted residue) increases with incresing S content of specimen. But the amount of sulfide is hardly varied by increasing Mn content from 0.5 to 1% for a constant S content. From this fact and the cracking test results, it can be concluded that the amount of MnS gives a little effect on cracking sensitivity.

S concentration in ferrite matrix was calculated by subtrating S concentration in MnS from bulk S content. S concentration in matrix is shown in Table 13. Except for No.1 specimen, the S concentration are constant as about 0.006 and 0.01, respectively for 1%Mn steels and 0.5%Mn steels. That is, the S concentration in matrix of 0.5%Mn steels is twice as much as that of 1%Mn steels. This fact suggests that a greater amount of dissolved S, which can

Table 12 Chemical compositions of steels used [24] (wt%)

No.	C	Si	Mn	S	Cr	Mo
1	0.19	0.24	0.43	0.019	1.03	0.55
2	0.17	0.49	0.55	0.030	1.07	0.51
3	0.20	0.19	0.41	0.054	1.06	0.57
4	0.21	0.24	0.52	0.092	1.16	0.54
5	0.18	0.36	1.14	0.016	1.07	0.51
6	0.18	0.52	1.23	0.028	1.11	0.52
7	0.18	0.41	1.12	0.049	1.16	0.52
8	0.22	0.36	1.13	0.093	1.13	0.53

Table 13 Results of electrolytic extraction and X-ray analyses [24]

steel			residue	sulfide	sol.S
No.	%Mn	%S	(wt%)	type	(wt%)
1	0.43	0.019	0.030	MnS	0.008
2	0.53	0.030	0.052	MnS	0.011
3	0.41	0.054	0.112	MnS	0.013
4	0.52	0.092	0.219	MnS	0.012
5	1.14	0.016	0.027	MnS	0.006
6	1.23	0.028	0.065	MnS	0.004
7	1.12	0.049	0.114	MnS	0.007
8	1.13	0.093	0.235	MnS	0.007

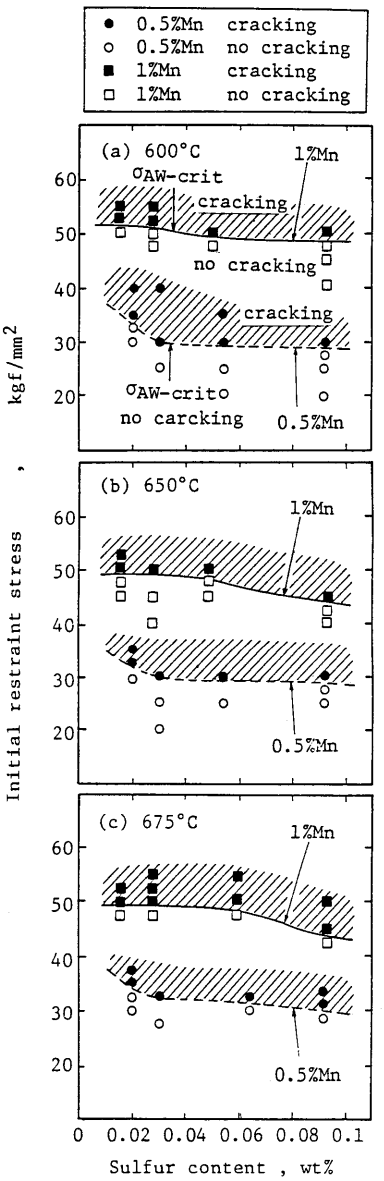

Fig.29 Influence of S on the critical restraint stress at holding temperature of 600, 650 and 675°C [24]

segregate at grain boundary and embrittles it, is present in the steels of lower Mn content.

4.2 Combined effect of REM and S

Nakao and Shinozaki et al. [25] investigated the effect of REM on the cracking sensitivity of 1Cr-0.5Mo and T-1 type high strength steels containing REM in a range of 0 to 0.17%, employing the hot tensile test at 600°C and y-slit crack test. REM increases the reduction of area and decreases the area fraction of reheat cracking as shown in Fig.30. This beneficial effect of REM is brought by the effect that REM fixes impurity elements, such as S and P, as inclusions and decreases soluble impurity, which may segregate to grain boundary and embrittle it.

Fujii and Yamamoto et al.[26] examined the effect of Ce on cracking sensitivity of HT80 (0.8%Ni-0.5%Cr-0.6%Mo) by using a constant-load type cracking test. Ce decreases the cracking sensitivity, even though the steel contains B which intensively increases the sensitivity, as shown in Fig.31.

4.3 Combined effect of Ca and S

Ohno and Okumura et al. [27] examined the combined effect of Ca and S in a

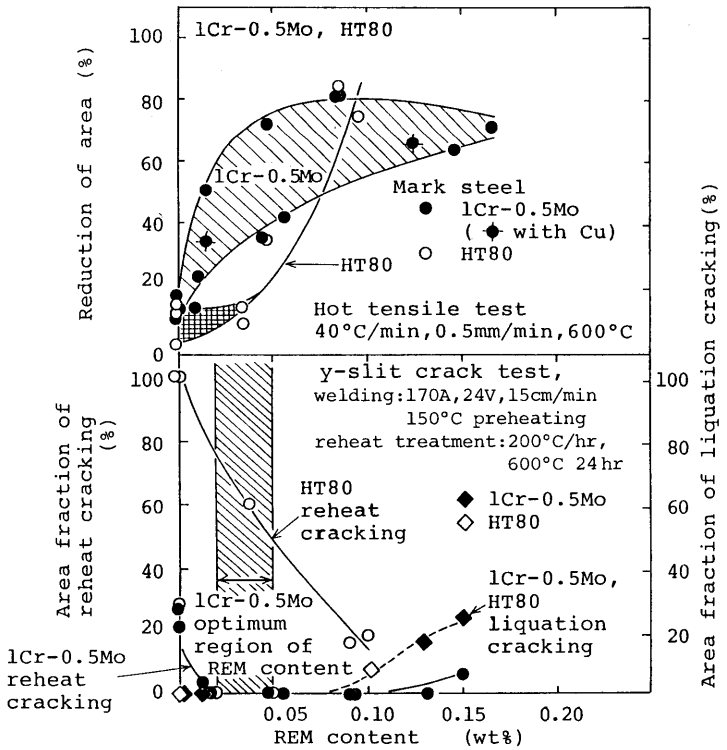

Fig.30 Effects of REM content on area fraction of reheat cracking and liquation cracking in small-sized y-slit crack test and reduction of area in hot tensile test of 1Cr-0.5Mo and HT80 steels [25]

HT80 steel by the cracking test with a saw-cut y-groove restraint specimen. The chemical compositions of steel specimens are: 0.11%C, 0.9%Mn, 0.013%P, 0.002 and 0.005%S, 0.70%Cr, 0.412%Mo,0 to 0.0039%Ca. The test results are shown in Fig.32. Percentage of crack decreases with increasing the Ca/S ratio for high S and low S steels. They assume that all Ca would combine with S to produce CaS and then remaining S would combine with Mn to produce MnS. MnS would be dissolved into matrix by weld thermal cycle. Dissolved S expressed by $S_{free}=S_{total}-(32/40)Ca$ is shown in Fig.33. Reheat cracking occurs when the dissolved S exceeds a critical value, which will depend on restraint intensity and chemical compositions of steel.

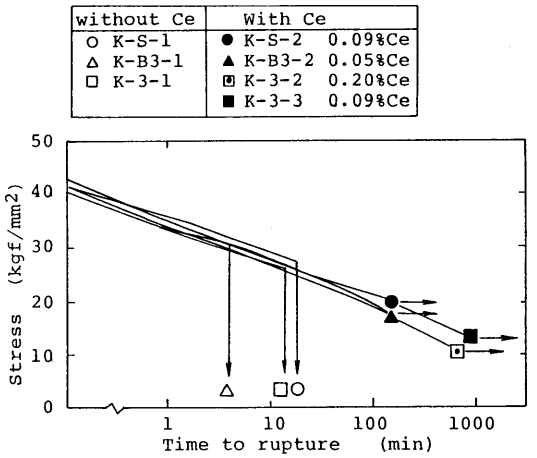

Fig.31 Effect of Cr on the supceptibility to rupture at 610°C (constant displacement)
Note: additional elements; K-3 basic composition(0.003%S,0.001%P), K-S 0.015%S, K-B3 0.0015%B [26]

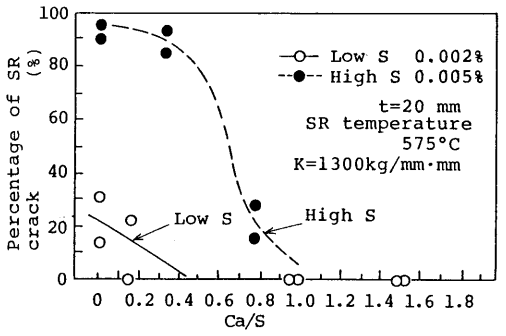

Fig.32 Relationship between Ca/S and percentage of SR crack (y-groove restraint SR cracking test) [27]

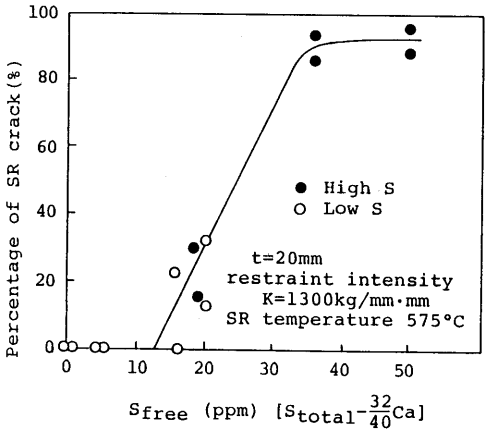

Fig.33 Relationship between S_{free} and percentage of SR crack [27]

5. Effects of other elements

5.1 Effect of Si and Al

Morishige and Okabayashi [28] examined the effects of Si and Al in 2 1/4Cr-1Mo and 1Cr-1/2Mo steels (Table 14). Weld thermal cycle was given on a cylinder type cracking test specimen shown in Fig.34. Restraint stress was loaded by welding a slit of the specimen as shown in the figure. As the results, the crack-initiating period is shown in Fig.35 (a) and (b). Those figures show that reheat cracking occurs in an earlier period with increasing the sol.Al content. Si shortens the crack-initiating period with decreasing its content down to 0.05%; but it extends the period when its content is smaller than 0.05%.

5.2 Effect of C

Kanazawa and Yamato [28] investigated the effect of several alloying elements and C on the cracking sensitivity of HT80 steels by using a multi-pass weld specimen. They informed that C increases the cracking sensitivity with increasing its content from about 0.10 to 0.12%. Other results on Cr, Mo, V, Nb and Cu are similar as those by other researchers. The result on Mn is similar as that of [27].

6. Conclusions

On the basis of the informations available at present time, the following conclusions can be drawn on the effect of several elements on the reheat cracking sensitivity of Cr-Mo steels.

(1) The cracking sensitivity of Cr-Mo steels varies remarkably depending on each set of Cr-Mo contents. The Cr-Mo contents-ΔAW-crit diagrams proposed recently will be beneficial for comparing the cracking sensitivity of those steels.

(2) The magnitudes of effects of minor alloying elements, V, Ti and Nb, and impurity elements, P, Sb, Sn, As and S, are dependent largely on each set of Cr-Mo contents.

(3) The tolerable limit of P content, Pcrit has been clarified for each set of Cr-Mo content.

(4) A tolerable limit of the total content of four impurity elements, P, Sb, Sn and As, Imp-crit, will be decided for each set of Cr-Mo contents in future. The concept of $\overline{X}$ parameter or P equivalent may be helpful for deciding Imp-crit value.

(5) For discussing the effect of another impurity element, S, the combined effects of S and the sulfide forming elements, Mn, Ca and REM, should be considered.

The authors of this report express their thanks to the original authors of each contribution and also to The Committee of Welding Metallurgy, Japan Welding Society for offering their valuable informations on the problem of reheat cracking.

Table 14 Chemical compositions of A508Cl.2 [28]

steel	C	Si	Mn	P	S	Cu	Ni	Cr	Mo	Sol.Al	N	O
a2	0.21	0.009	0.72	0.011	0.007	0.10	0.82	0.36	0.62	0.003	0.004	0.003
a3	0.20	0.007	0.71	0.007	0.010	0.09	0.81	0.35	0.61	0.023	0.004	0.002
a5	0.21	0.06	0.71	0.007	0.010	0.10	0.81	0.36	0.61	0.006	0.004	0.002
a7	0.18	0.33	0.68	0.007	0.009	0.10	0.81	0.35	0.60	0.007	0.004	0.002

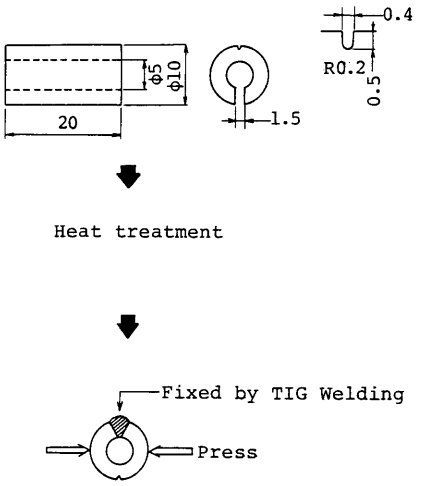

Fig.34 Cylinder type restraint SR cracking test specimen [28]

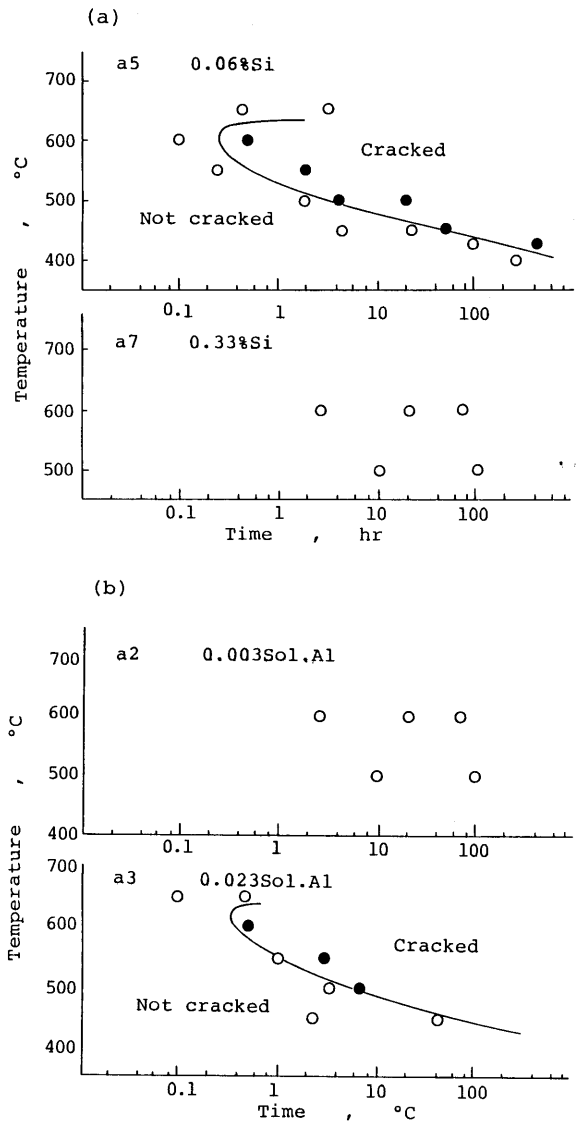

Fig.35 SR cracking test results for 4 kinds of A508 cl.2 steels [28]

References

1) R.W.Nichols: IIW Doc.X-547-69, IX-665-69 (1969)
2) T.Naiki and H.Okabayashi: J. of JWS,39-10,1059-1066(1970)[in Japanese]
3) Y.Itoh and M.Nakanishi: J.of JWS,41-1,59-64(1972)[in Japanese]
4) K.Watanabe and S.Kirihara: Preprints of the national meeting of JWS, No.18,84-85(1976)[in Japanese]
5) K.Tamaki and J.Suzuki: Trans. JWS,14,117-122(1983)
6) K.Tamaki and J.Suzuki: Trans. JWS,14,123-127(1983)
7) K.Tamaki and J.Suzuki: Trans. JWS,16,117-124(1985)
8) K.Tamaki, J.Suzuki and M.Tajiri: Trans. JWS,15,17-24(1984)
9) K.Tamaki, J.Suzuki and Y.Nakaseko: Trans. JWS,15,8-16(1984)
10) T.Kikuchi and I.Ohnishi: J.JWS,47-2,85-92(1978)[in Japanese]
11) T.Kikuchi and I.Ohnishi: Trans. JIM,19,341-350(1978)
12) T.Kikuchi and I.Ohnishi: J.JWS,47-9,632-638(1978)[in Japanese]
13) T.Kikuchi and I.Ohnishi: Trans. JIM,19,351-361(1978)
14) T.Kikuchi and I.Ohnishi: J.JWS,48-10,838-845(1979)[in Japanese]
15) T.Kikuchi and Y.Nakao : 4th Int.Sympo.JWS,(Nov.,Osaka)455-460(1982)
16) T.Matsuzaka, S.Kirihara et al.: J.JWS,51-1,58-63(1982)[in Japanese]
17) R.Bruscato: Welding J.,49-4,148s-156s(1970)
18) H.Ikawa, Y.Nakao et al.: J.JWS,47-3,153-160(1978)[in Japanese]
19) H.Ikawa, Y.Nakao et al.: J.JWS,47-7,425-432(1978)[in Japanese]
20) H.Ikawa, Y.Nakao et al.: J.JWS,49-2,136-142(1980)[in Japanese]
21) D.McLean:Grain boundaries in metal,Oxford (1957)
22) Y.Nakao and T.Nishiyama: J.JWS,49-12,835-839(1980)[in Japanese]
23) Y.Nakao and T.Nishiyama: J.JWS,50-7,663-668(1981)[in Japanese]
24) K.Tamaki, J.Suzuki et al.: Preprints of National Meeting of JWS, No.39(1986)[in Japanese]
25) Y.Nakao, K.Shinozaki et al.: Preprints of National Meeting of JWS, No.35,164(1984)[in Japanese]
26) T.Fujii, K.Yamamoto et al.: Testu to Hagane, 69-9,1777-1785(1981) [in Japanese]
27) Y.Ohno, Y.Okumura et al.: Testu to Hagane,67-10,121-130(1981)[in Japanese]
28) T.Morishige and H.Okabayashi: Preprints of the National Meeting of JWS, No.31,72-73(1982)[in Japanese]
29) S.Kanazawa, K.Yamato et al.: J.JWS,44-10,791-798(1975)[in Japanese]